Pergamon

SCIENCE DIRECT®

Bioorganic & Medicinal Chemistry 11 (2003) 21–29

BIOORGANIC & MEDICINAL CHEMISTRY

Crystal Structures of Reversible Ketone-Based Inhibitors of the Cysteine Protease Cruzain

Lily Huang,[a] Linda S. Brinen[b,*,†] and Jonathan A. Ellman[a,*]

[a]*Center for New Directions in Organic Synthesis, Department of Chemistry, University of California, Berkeley, CA, 94720, USA*
[b]*Department of Pathology, University of California, San Francisco, CA 94143, USA*

Received 28 May 2002; accepted 8 August 2002

Abstract—The crystal structures of two hydroxymethyl ketone inhibitors complexed to the cysteine protease cruzain have been determined at 1.1 and 1.2 Å resolution, respectively. These high resolution crystal structures provide the first structures of non-covalent inhibitors bound to cruzain. A series of compounds were prepared and tested based upon the structures providing further insight into the key binding interactions.

Introduction

Infection by the protozoan parasite *Trypanosoma cruzi* results in Chagas' disease, which is the principal cause of heart disease in South America.[1] The only currently available treatment is insufficient due to considerable toxicity.[2] The lack of effective treatment has stimulated efforts to identify novel drug targets against this parasite. One target that has received significant attention is cruzain, the major cysteine protease found in *T. cruzi*. Recently, McKerrow et al. have shown that irreversible inhibitors of cruzain can cure parasitic infections in mouse models.[3] These results demonstrate the therapeutic promise of inhibitors of cruzain for the treatment of Chagas' disease.

Knowledge of the high-resolution structure of a target protease significantly facilitates the design of potent and selective inhibitors. Previous crystal structures of cruzain complexed with irreversible inhibitors have provided useful information about the binding interactions of inhibitors with cruzain. McGrath et al. reported the first crystal structure of cruzain in 1995.[4] In this 2.35 Å structure, the active-site cysteine of cruzain was irreversibly alkylated with Cbz-Phe-Ala-fluoromethyl ketone. In a later study, Gillmor et al. reported the structures of cruzain complexed to Cbz-Arg-Ala-fluoromethyl ketone and Cbz-Tyr-Ala-fluoromethyl ketone at 2.2 and 2.1 Å resolution, respectively.[5] These structures provided a structural basis for the binding specificity of the P_2 substituent, which is often a critical specificity determinant for cysteine proteases. In particular, these structures revealed that cruzain is able to accommodate both hydrophobic and basic residues in the P_2 position by a rotation of the Glu205 residue, which is found at the bottom of the S_2 pocket. More recently, four high-resolution crystal structures of cruzain bound to vinyl sulfone derivatives were reported (resolution ranged from 1.6 to 2.15 Å).[6] As expected, the mode of inhibition was a Michael addition between the active site Cys25 and the vinyl sulfone.

We have recently reported a series of highly potent and selective reversible inhibitors of cruzain.[7] We focused on developing reversible inhibitors in order to minimize the toxicity that can be observed with irreversible inhibitors.[3b] Our efforts have also led to the identification of hydroxymethyl ketone analogues that are moderately potent inhibitors of cruzain. Herein, we report a 1.1 Å crystal structure of hydroxymethyl ketone **1** complexed to cruzain and a 1.2 Å crystal structure of hydroxymethyl ketone **2** complexed to cruzain. These high-resolution results represent the first reported X-ray structures of cruzain bound to non-covalent inhibitors.

*Corresponding author. Fax: +1-510-642-8369; e-mail: jellman@uclink.berkeley.edu
†Present address: Joint Center for Structural Genomics, Stanford University, 2575 Sand Hill Road, SSRL MS69, Menlo Park, CA 94025, USA.

0968-0896/03/$ - see front matter © 2002 Elsevier Science Ltd. All rights reserved.
PII: S0968-0896(02)00427-3

Crystal Structures Results and Discussion

The crystal structures of the two inhibitors **1** and **2** (Fig. 1), respectively, show very similar modes of binding. When the structures of **1** bound to cruzain and **2** bound to cruzain (from here on abbreviated as **cruz-1** and **cruz-2**, respectively) are aligned and superimposed, they show a high degree of similarity to one another (Table 1 and Fig. 2). In both structures, no covalent bond is formed between the active-site cysteine and the ketone pharmacophore, as is evidenced by a clear gap in the experimental electron density between the two moieties. In fact, the ketone moiety and Cys25 are oriented in conformations that are incompatible with covalent bond formation (Fig. 3). In contrast, the ketone carbonyl is stabilized through a set of hydrogen-bonding interactions with Gln19 and Cys25. Contacts between Gln19 Nε and the carbonyl oxygen are 3.11 and 3.15 Å for **cruz-1** and **cruz-2,** respectively. Contacts between the S of Cys25 and the carbonyl oxygen are 3.11 and 3.08 Å for **cruz-1** and **cruz-2**, respectively.

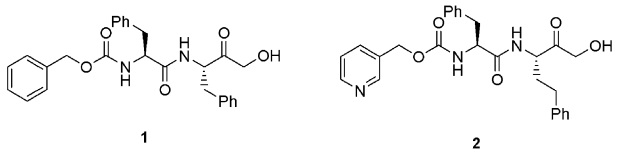

Figure 1. Hydroxymethyl ketone inhibitor structures and K_i values.

Table 1. Data collection and refinement statistics

Crystal and diffraction data	cruz-1	cruz-2
Unit-cell dimensions:		
a (Å)	42.52	42.57
b (Å)	51.71	51.59
c (Å)	46.04	45.95
β (°)	116.53	116.62
Space group	$P2_1$	$P2_1$
Data Collection Statistics		
Resolution limit (Å)	1.1	1.2
Total number of reflections collected	440603	252261
Number of unique reflections ($F > 0\sigma\|F\|$)	53954	43377
R_{merge} (%)[a]	0.034	0.030
R_{merge} on highest resolution bin of data	0.13	0.065
Completeness		
Overall (%)	96.4	99.1
Highest resolution shell (%)	91.1	97.8
Refinement statistics		
Resolution range (Å)	30–1.2	30–1.2
R_{cryst}[b]	0.0969 for 52264 refl	0.0939 for 42575 refl
R_{free}[c]	0.130 for 1631 refl	0.135 for 4792 refl
R_{msd}		
Bond lengths (Å)	0.016	0.011
Bond angles (°)	0.031	0.029
From flat planes	0.0297 for 1309 atoms	0.0295 for 1309 atoms
Water molecules	484	551
Average B factor (Å^2)		
All atoms	15.01	13.45
Protein	8.44	8.04
Inhibitor	14.48	16.10
Water	35.15	28.44
RMSD of superimposed complex (cruzain + inhibitor) structures		
All backbone atoms (860 atoms)	0.11 Å	
All atoms (1591 atoms)	0.41 Å	
All side-chain atoms (792 atoms)	0.59 Å	

[a] $R_{merge} = \left(\sum_h \sum_i \left| \left(I_{hi} - \left\langle I_h \right\rangle \right) \right| \right) / \sum_h I$ where I_h is the mean structure—factor intensity of i observations of symmetry-related reflections with Bragg intensity index h.

[b] $R_{cryst} = \left(\sum_h \sum_i \| F_{obs}| - |F_{calc} \| \right) / \sum |F_{obs}|$ where F_{obs} and F_{calc} are the observed and the calculated structure factor magnitudes.

[c] $R_{free} = \sum_{(hkl)\tau} \| F_{obs(hkl)}| - k|F_{(hkl)}| / \sum_{(hkl)} \tau |F_{obs(hkl)}|$ where the τ set of reflections is omitted from the refinement process; 10% of the data were included in the τ set.

Both inhibitors contained a phenylalanine residue in the P_2 position. Similar to previously published crystal structures, the S_2 pocket was defined by the hydrophobic residues Leu67, Ala133 and Leu157. As expected, the Glu205 residue at the bottom of the S_2 pocket was rotated away from the hydrophobic phenylalanine side chain.

The inhibitor backbone is stabilized by a series of hydrogen bonds with the Gly66 residue. In the **cruz-1** structure, the distance between the amide NH of Gly66 and the carbonyl of the P_2 phenylalanine residue is 3.08 Å. The amide NH of the P_2 residue shows a distance of 3.18 Å with a nearby water molecule. This amide NH

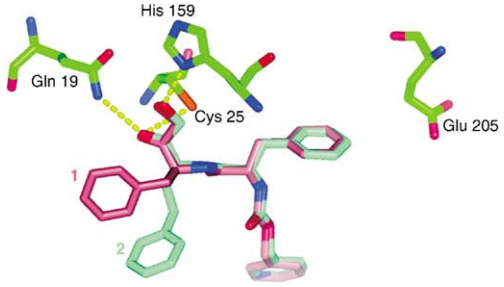

Figure 2. Cruzain's active site, shown in cartoon, with superimposed **1** (salmon) and **2** (aqua) inhibitor molecules. Hydrogen bond interactions described in the text are shown. Figure prepared with PyMOL.

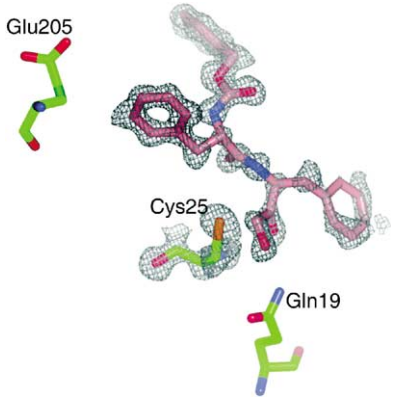

Figure 3. Electron density at 1.0 sigma (3Fo-2Fc) is shown for inhibitor **1** and the side chain of Cys25. A gap between the protein and inhibitor is visible. The high B-factor values for the Phe of 1 result in noncontinuous electron density for this moiety. Figure prepared with PyMOL.

also shows a potential interaction with the cruzain main chain carbonyl of Asp158. In addition, this NH is 2.81 Å away from the carbonyl of Gly66. The carbamate carbonyl interacts with two water molecules at distances of 2.75 and 3.14 Å away. In the **cruz-2** structure, contacts between the amide N of Gly66 and the carbonyl of the P2 phenylalanine residue is 3.07 Å. The amide NH of the P_2 residue is 3.0 Å away from a nearby water molecule. In addition, this NH is 2.74 Å away from the carbonyl of Gly66. The carbamate carbonyl interacts with a water molecule at 2.74 Å and the pyridinyl N shows a potential interaction with the hydroxyl group in Ser61.

Interestingly, both crystal structures showed a strong hydrogen bond between His159 (part of the canonical catalytic triad, Cys25, His159 and Asn175, of this family of cysteine proteases) and the hydroxyl group in the inhibitor. These hydrogen bond distances are 2.68 and 2.50 Å for the **1** and **2** inhibitors, respectively. This type of hydrogen bond interaction has not been previously observed in similar cysteine protease crystal structures.

The homophenylalanine (hPhe) residue in the P_1 position of **2** extends into the solvent and does not make productive interactions with the enzyme. The hPhe residue was initially chosen since researchers observed that incorporation of the hPhe side chain at P_1 resulted in inhibitors that were not degraded by human proteases, in contrast to the corresponding inhibitors that incorporate natural amino acids in this position.[8] This replacement also reduced the toxicity of vinyl sulfone inhibitors in animal studies.[9] The high B-factor seen in this position shows that this is a good position for further modification. Preliminary docking studies suggest that changing the hPhe side chain to a butyl or hydroxypropyl group may improve the interactions with the enzyme while reducing the molecular weight of the inhibitors.

Evaluation of inhibitor with a thiol group replacing the hydroxyl group

To probe the importance of the hydrogen bonding interaction between the hydroxyl group of inhibitors **1** and **2** and the active site imidazole, the hydroxyl group was replaced with a thiol group. Surprisingly, inhibitor **3** showed greater than 15-fold improvement in inhibitory activity despite the generally reduced hydrogen bonding potential of a thiol versus an alcohol. The potency of inhibitor **3** could possibly result from disulfide bond formation with the active site cysteine thiol. To test this possibility the assay was performed under different redox conditions by varying the concentration of DTT (1–10 mM). However, the inhibitory activity of inhibitor **3** was independent of DTT concentration implying that the potency of this compound is not due to disulfide bond formation.

Evaluation of inhibitors lacking the ketone pharmacophore

The crystal structures of complexes of inhibitors **1** and **2** show that the enzyme makes a number of hydrogen bonds to the ketone carbonyl. However, the active site thiol does not form a covalent bond with the ketone pharmacophore. We therefore chose to replace the ketone carbonyl with a methylene group to provide inhibitor **4** (Table 2), since the carbonyl has the potential to result in toxicity and unfavorable pharmacokinetics. No inhibition was observed even at 10 μM concentrations of **4,** clearly indicating the importance of the hydrogen bonding interactions with the ketone pharmacophore.

Table 2. Cruzain inhibition data

Compd	Structure	Cruzain K_I (nM)[a]
3	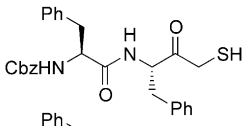	4.4±0.9
4	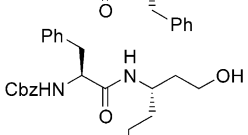	>10,000
5	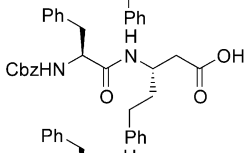	>10,000
6	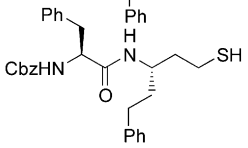	>5000

[a] K_i values determined at four to eight concentrations in duplicate using the linear regression analysis of Williams and Morrison.[14]

A series of compounds was prepared in an attempt to improve the inhibitory activity of compounds lacking the ketone pharmacophore. First, inhibitor **5** was synthesized with a carboxylic acid group in place of the hydroxyl group, since the carboxylic acid should provide a stronger hydrogen bonding interaction with the active site imidazole. However, no improvement in the inhibitory activity of **5** was observed. Inhibitor **6** with a thiol group in place of the hydroxyl group was also prepared, since the corresponding substitution to provide the ketone inhibitor **3** resulted in a dramatic improvement in activity (vide infra). Unfortunately, inhibitor **6** showed only a modest 5 μM inhibition.

Inhibitor synthesis

The *N*-Cbz-Phe-Phe hydroxymethyl ketone (**1**) was synthesized as summarized in Scheme 1. The commercially available *N*-Cbz-Phe-Phe dipeptide **7** was converted to the bromomethyl ketone dipeptide **8** in a one-pot procedure.[10] Displacement of the bromomethyl ketone with benzoylformic acid,[11] followed by hydrolysis of the formate ester **9** with aqueous potassium bicarbonate afforded the desired hydroxymethyl ketone **1**.

The 3-pyridinylmethoxycarbonyl-Phe-hPhe hydroxymethyl ketone **2** was synthesized as shown in Scheme 2.

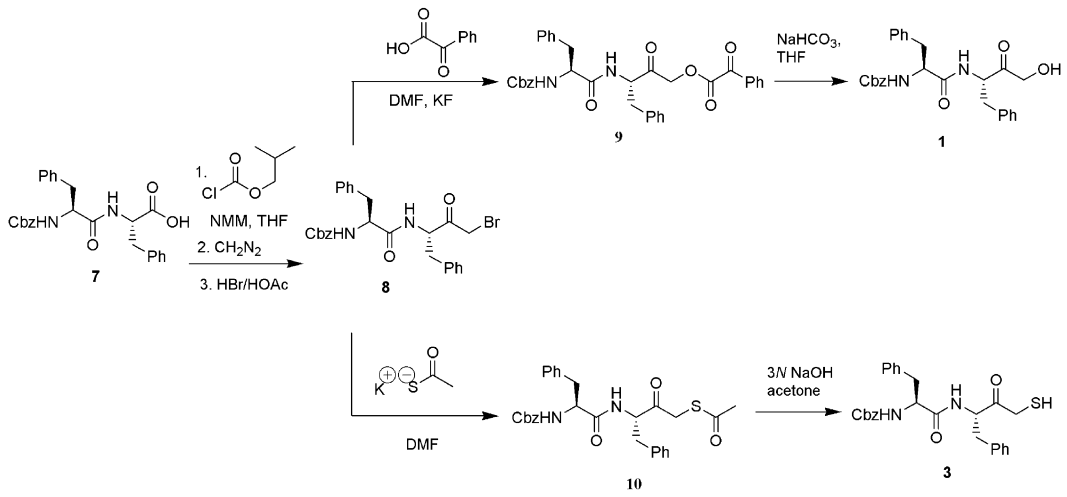

Scheme 1. Synthesis of hydroxymethyl ketone **1** and mercaptomethyl ketone **3**.

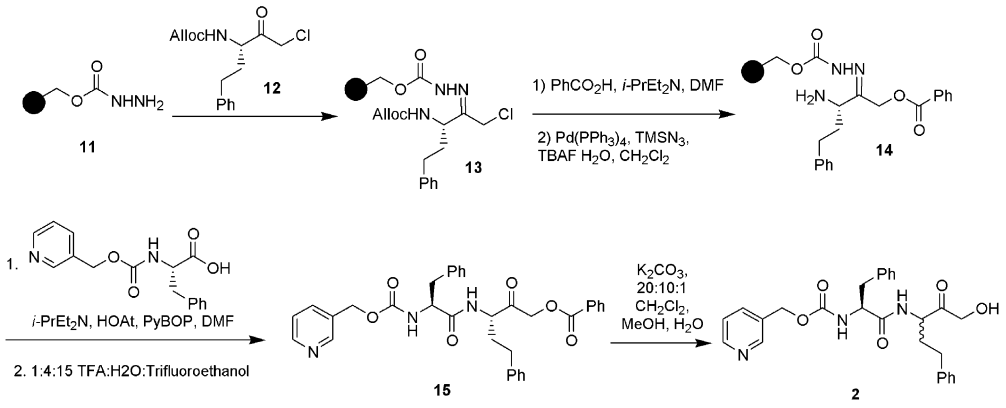

Scheme 2. Synthesis of hydroxymethyl ketone **2**.

The acyloxymethyl ketone analogue **15** was synthesized using a previously reported solid-phase strategy.[12] The benzoate was then hydrolyzed under basic conditions to afford the hydroxymethyl ketone **2**.

The sulfhydryl ketone **3** was synthesized by displacement of **8** with potassium thiolate to afford the thioester **10** (Scheme 1). The thioester was hydrolyzed under rigorous oxygen-free and moisture-free conditions to prevent oxidation and decomposition of the thiol.

The analogues lacking the ketone pharmacophore were synthesized using *tert*-butanesulfinamide **16** as a chiral auxiliary (Scheme 3). *tert*-Butanesulfinamide was condensed with hydrocinnamaldehyde to give the *tert*-butanesulfinyl imine **17**. Addition of a titanium enolate

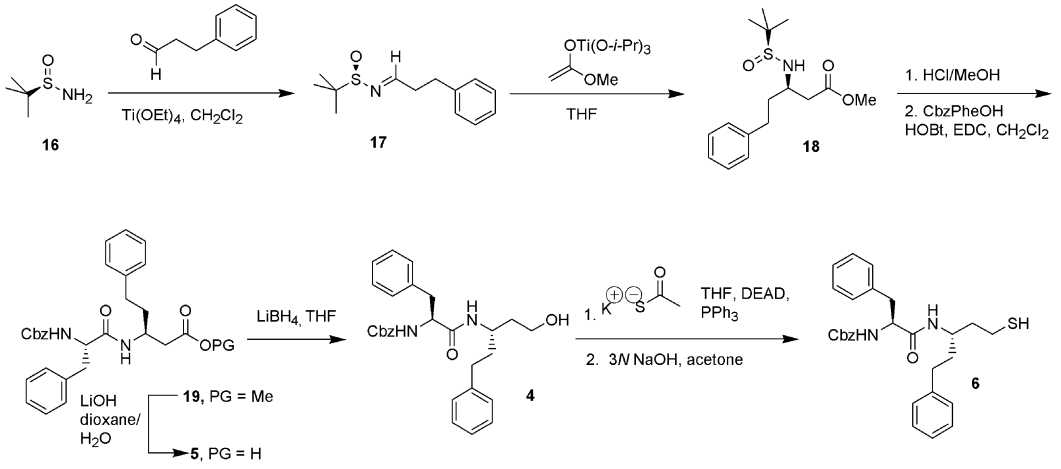

Scheme 3. Synthesis of inhibitors lacking the ketone pharmacophore.

of methyl acetate to **17** gave the chiral product **18**. Cleavage of the *N*-*tert*-butanesulfinyl group followed by acylation with *N*-Cbz-Phe-OH gave the methyl ester intermediate **19**. Reduction with $LiBH_4$ resulted in selective reduction of the methyl ester to the primary alcohol **4** without reduction of the amide bond.

The analogous sulfhydryl inhibitor **6** was synthesized from alcohol **4** (Scheme 3). A Mitsunobu reaction of thioacetic acid and alcohol **4** provided an intermediate thioester that was hydrolyzed under rigorous oxygen-free conditions to prevent oxidation of the liberated thiol. Finally, the carboxylic acid inhibitor **5** could be prepared by saponification of the methyl ester intermediate **19**.

Conclusions

We have reported two very high resolution crystal structures of two hydroxymethyl ketones **1** and **2** bound to cruzain. These crystal structures provide valuable insight into the binding of these mechanism-based inhibitors to the enzyme active site. In particular, these crystal structures show that the active site cysteine thiol does not form a covalent bond with the ketone pharmacophore. In addition, the structures show a strong hydrogen bond between the active site imidazole and the hydroxyl group of the inhibitor. A series of second generation compounds were prepared and tested providing further insight into the key binding interactions.

Experimental

General methods

Unless otherwise noted, all reagents were obtained from commercial suppliers and used without further purification. THF was distilled under N_2 from sodium/benzophenone, and CH_2Cl_2 and *i*-Pr_2EtN were distilled over CaH_2 immediately prior to use. ArgoGel-OH resin was purchased from Argonaut Technologies (San Carlos, CA, USA). Reaction progress was monitored through thin-layer chromatography on Merck 60 F_{254} 0.25 mm silica plates. Unless otherwise specified, extracts were dried over $MgSO_4$ and solvents were removed with a rotary evaporator at aspirator pressure. All compounds were purified by flash chromatography using Merck 60 230–400 mesh silica gel. Infrared spectra were recorded with a Perkin-Elmer 1600 series Fourier transform spectrometer as thin films on NaCl plates and only partial data are listed. ^1H and ^{13}C NMR spectra were obtained with Bruker AMX-300 and DRX 500 spectrometers. Unless otherwise specified, all spectra were obtained in $CDCl_3$; chemical shifts are reported in parts per million relative to TMS, and coupling constants are reported in Hertz. HRMS analysis was performed at the UC Berkeley Mass Spectrometry Facility.

Compound 1. A solution of *N*-Cbz-Phe-Phe-OH dipeptide (2.00 g, 4.47 mmol) in 6 mL of THF was immersed in a dry ice/acetonitrile bath at −25 °C with stirring under a N_2 atmosphere. To this solution was added sequentially 4-methyl morpholine (0.69 mL, 6.3 mmol, 1.4 equiv) and isobutyl chloroformate (0.75 mL, 5.8 mmol, 1.3 equiv). The latter was added dropwise and resulted in the immediate formation of white solid. The reaction mixture was stirred vigorously, and the bath maintained at a temperature around −25 °C. After 1 h, the reaction mixture was filtered and the solid was rinsed with ice-cold THF. Rinses were added to the solution, which was stirred again at −25 °C. Additional THF for rinsing was added until the concentration was no lower than 0.2 M. Diazomethane was introduced in situ using Diazald (2.97 g, 13.9 mmol, 3.1 equiv), and the reaction flask was maintained at −25 °C for 30 min once addition was complete. The solution was allowed to warm to rt for 30 min before immersion in an ice water bath. A mixture of 1:1 48% HBr/glacial acetic acid was added dropwise until bubbling ceased. The solvent was evaporated and the pale yellow/orange crude product was dissolved in ethyl acetate. The organic layer was washed with water and then with saturated $NaHCO_3$ until rinses were no longer acidic. The organic layer was dried, the solvent removed and the crude product was recrystallized in absolute ethanol.

To a solution of bromomethyl ketone **8** (0.100 g, 0.191 mmol) in 2 mL of DMF was added benzoyl formic acid (0.034 g, 0.229 mmol, 1.2 equiv) and potassium fluoride (0.017 g, 0.287 mmol, 1.5 equiv). This yellow solution was stirred overnight at rt. This solution was diluted with 5 mL of EtOAc and 2.5 mL of water. The organic layer was washed with saturated NaCl, dried with $MgSO_4$ and concentrated to form a yellow-white solid. To a solution of unpurified **9** in 10 mL of THF was added 10 mL of a 1 M solution of $NaHCO_3$. This reaction mixture was stirred overnight, resulting in a cloudy white solution. This solution was diluted in EtOAc and washed with water, saturated NaCl, dried with $MgSO_4$ and concentrated to give the desired product **1** as a white solid 65.6 mg (75%). A portion of the product was chromatographed (~2 mL of silica and a solvent gradient of 4:1 hexanes/ethyl acetate to 1:1 hexanes/ethyl acetate) to ensure complete purity, providing 13 mg of product **1** for biochemical analysis. IR: 1658, 1687, 1726, 3292 cm^{-1}. ^1H NMR (500 MHz): δ 2.89–3.01 (m, 4H), 3.94 (d, 1H, $J = 19.5$ Hz), 4.07 (d, 1H, $J = 19.5$ Hz), 4.35–4.40 (m, 1H), 4.75 (m, 1H), 5.07 (s, 2H), 5.22 (d, 1H, $J = 7.5$ Hz), 6.33 (d, 1H, $J = 7.0$ Hz), 6.95–7.38 (m, 15H). ^{13}C NMR (125 MHz): δ 30.3, 37.4, 38.0, 56.0, 56.1, 67.4, 127.3, 127.4, 128.1, 128.3, 128.6, 128.8, 128.9, 129.0, 129.2, 135.0, 135.9, 135.9, 155.9, 170.8, 208.0. FABHRMS: 461.2076 (MH^+, $C_{27}H_{28}N_2O_5$ requires 461.2081).

Compound 2. Using a previously reported solid-phase strategy,[12] an acyloxymethyl ketone derivative of *N*-[(3-pyridinyl)methoxycarbonyl]-Phe-hPhe (**15**) was synthesized. Acyloxymethyl ketone **15** was purified via column chromatography (~2 mL of silica and a solvent gradient from 4:1 hexanes/ethyl acetate to 100% ethyl acetate) in a 60% yield. The acyloxymethyl ketone was subsequently hydrolyzed under the following basic conditions.[13] In a Schlenk flask, **15** (78 mg, 0.13 mmol) was

dissolved in 4 mL of a 20:10:1 solvent mixture of CH_2Cl_2/MeOH/H_2O and subjected to three freeze—pump—thaw cycles. Oxygen-free conditions were required to prevent oxidation of the resulting hydroxymethyl ketone **2**. Under positive N_2 pressure, K_2CO_3 (0.10 g, 0.72 mmol) was added to the reaction mixture and stirred under N_2 for 3.5 h. The resulting solution was diluted with 10 mL of EtOAc and 5 mL of water in a separatory funnel. The layers were separated and the organic layer was further washed with sat. NaCl, dried with $MgSO_4$ and concentrated. Purification by column chromatography (~2 mL of silica and a solvent gradient of 4:1 hexanes/ethyl acetate to 100% ethyl acetate) afforded the white solid in a 49% unoptimized yield (31.5 mg). IR: 1658, 1690, 1723, 3293 cm^{-1}. ^1H NMR (300 MHz): δ 1.56–1.87 (m, 1H), 1.94–2.17 (m, 1H), 2.34–2.39 (m, 1H), 2.49–2.54 (m, 1H), 3.03–3.07 (m, 2H), 4.18–4.27 (m, 2H), 4.42–4.52 (m, 1H), 4.57 (m, 1H), 4.99–5.10 (m, 2H), 5.61–5.88 (m, 1H), 6.71–6.86 (m, 1H), 7.02–7.33 (m, 11H), 7.58–7.61 (m, 1H), 8.51–8.54 (m, 2H). ^{13}C NMR (125 MHz): δ 31.3, 32.6, 38.1, 54.8, 56.4, 64.4, 66.6, 123.5, 126.4, 127.2, 128.3, 128.5, 128.8, 129.2, 131.8, 131.9, 136.1, 140.1, 140.2, 149.0, 155.7, 171.2, 208.1. FABHRMS: 476.2185 (MH^+, $C_{27}H_{29}N_3O_5$ requires 476.2176).

Compound 3. To a solution of bromomethyl ketone **8** (0.100 g, 0.191 mmol) in 2 mL of DMF was added potassium thioacetate (0.024 g, 0.210 mmol, 1.1 equiv). This cloudy orange-yellow solution was stirred overnight at rt. This solution was diluted with 10 mL of EtOAc and 5 mL of water. The organic layer was washed with saturated NaCl, dried with $MgSO_4$ and concentrated to form 73.6 mg (74%) of the thioester **10**.

In a 25 mL flame-dried Schlenk flask, reagent grade acetone (5 mL) and 3 N NaOH (5 mL) were subjected to four freeze—pump—thaw cycles to form strict oxygen-free conditions. Under positive N_2 pressure, the crude compound **10** (0.1 g, 0.2 mmol) was added as a solid to the Schlenk flask. This reaction mixture was stirred under N_2 for 2 h. A solution of 1 M HCl was added to neutralize the solution, resulting in the formation of a brown precipitate. The aqueous layer was extracted with CH_2Cl_2 (3×5 mL) and the combined extracts were dried with $MgSO_4$ and concentrated to give 82.2 mg of brown solid. This solid was purified by column chromatography (~2 mL of silica and a solvent gradient from 4:1 hexanes:ethyl acetate to 100% ethyl acetate) to give 38.2 mg of product **3**. The major diasteromer is reported.

40% yield. IR: 1654, 1700, 1702 cm^{-1}. ^1H NMR (500 MHz): δ 2.82–3.18 (m, 6H), 4.37 (m, 1H), 4.92 (m, 1H), 5.08 (s, 2H), 5.19 (m, 1H), 6.34 (m, 1H), 7.01–7.36 (m, 15H). ^{13}C NMR (125 MHz): δ 32.8, 37.6, 38.2, 56.2, 57.7, 67.2, 127.1, 127.3, 127.3, 129.1, 128.3, 128.5, 128.8, 128.9, 129.1, 129.2, 135.4, 136.0, 155.9, 170.7, 203.5. FABHRMS: 477.1848 (MH^+, $C_{27}H_{28}N_2O_4S$ requires 477.1842).

Compound 17. In a flame dried 50-mL round-bottom flask, (*R*)-*tert*-butanesulfinamide (0.125 g, 1.14 mmol) was dissolved in 2 mL of CH_2Cl_2 and stirred under N_2. To this solution was added $Ti(OEt)_4$ (0.60 mL, 2.6 mmol, 2.3 equiv) and freshly distilled hydrocinnamaldehyde (0.16 mL, 1.2 mmol, 1.1 equiv). This solution was stirred at rt and under N_2 for 1.5 h. The solution was diluted threefold with CH_2Cl_2 and incubated with a 2:1 finely powdered mixture of sand/$Na_2SO_4 \cdot H_2O$ (5 g/mmol imine) for 1 h with occasional shaking by hand. Filtration, rinsing, and concentration led to the imine product **17** (0.27 g, 100%) as a light yellow oil. Imine **17** was generally used immediately in the next step.

Compound 18. In a 25-mL flame-dried round-bottom flask, diisopropyl amine (0.35 mL, 2.5 mmol, 2.2 equiv) was dissolved in THF (5.7 mL) and stirred at 0 °C under N_2. To this solution, *n*-BuLi (1.3 mL, 2.39 mmol, 2.1 equiv) was added dropwise. This solution was stirred at 0 °C for 20 min and then cooled to −78 °C. Anhydrous methyl acetate (0.18 mL, 2.3 mmol, 2 equiv) was added dropwise and the pale yellow reaction mixture was stirred for an additional 30–45 min. To this mixture was added a solution of $TiCl(O\text{-}i\text{-}Pr)_3$ (1.1 mL, 4.8 mmol, 4.2 equiv) in THF (1.1 mL), giving an opaque orange solution. After this solution was stirred at −78 °C for 35 min, a solution of imine **17** (1.1 mmol) in 2 mL of THF was added dropwise. This reaction mixture was then stirred at −78 °C for 2 h, followed by quenching with 2 mL of saturated NH_4Cl at −78 °C. A white precipitate immediately formed and the reaction mixture was allowed to warm up to rt before it was diluted with water and extracted with EtOAc (3×5 mL). The combined organic extracts were washed with saturated NaCl, dried with $MgSO_4$ and concentrated to give a yellow oil. The enolate addition product was purified by column chromatography (~20 mL of silica and a gradient column from 3:1 hexanes/ethyl acetate to 100% ethyl acetate) to afford 0.23 g (67%) of **18**.

^1H NMR (500 MHz): δ 1.26 (s, 9H), 1.82–1.96 (m, 2H), 2.60–2.87 (m, 4H), 3.54–3.60 (m, 1H), 3.68 (s, 3H), 4.27 (d, 1H, J=8.8 Hz), 7.16–7.30 (m, 5H). ^{13}C NMR (125 MHz): δ 22.7, 32.2, 37.3, 40.2, 51.7, 53.4, 56.0, 126.0, 128.4, 128.5, 141.3, 172.4.

Compound 19. The sulfinyl group in sulfinamide **18** (0.23 g, 0.76 mmol) was cleaved by addition of 4 N HCl solution in dioxane (0.4 mL, 1.5 mmol, 2 equiv) and an equal volume of MeOH, while stirring under N_2 in a cold water bath. After 30 min of stirring, the reagents/solvents were removed by passing N_2 over the solution. The resulting amine salts were re-dissolved in CH_2Cl_2 and free-based with Et_3N (0.21 mL, 1.5 mmol, 2 equiv). The organic layers were washed with water, saturated NaCl, dried with $MgSO_4$ and concentrated to give the free amine as a yellow oil.

The crude amine was dissolved in CH_2Cl_2 (3.8 mL, 0.2 M) and stirred in an ice bath. To this solution was added HOBt (0.21 g, 1.5 mmol, 2 equiv), *N*-Cbz-Phe-OH (0.25 g, 0.84 mmol, 1.1 equiv) and EDC (0.20 g, 1.1 mmol, 1.4 equiv). This reaction mixture was stirred for 2 h at 0 °C and then slowly warmed to rt overnight. After

this incubation period, the solution was diluted in CH_2Cl_2 and washed with 1 N HCl, saturated $NaHCO_3$ (2×5 mL), water, 1 N HCl (2×5 mL), and saturated NaCl. The organic layer was dried with $MgSO_4$, concentrated and purified through recrystallization in absolute ethanol to afford 0.23 g (61%) of **19**.

^{1}H NMR (500 MHz): δ 1.63–1.72 (m, 2H), 2.41–2.48 (m, 4H), 3.00–3.10 (m, 2H), 3.61 (s, 3H), 4.19 (m, 1H), 4.37 (m, 1H), 5.05–5.14 (m, 2H), 5.30 (m, 1H), 6.26 (d, 1H, J=9 Hz), 7.08–7.33 (m, 15H). FABHRMS: 489.2387 (MH^+, $C_{29}H_{32}N_2O_5$ requires 489.2389).

Compound 4. Ester **19** (0.16 g, 0.32 mmol) was dissolved in 1.6 mL of THF and stirred under N_2. $LiBH_4$ (0.48 mL, 0.96 mmol, 3 equiv) was added dropwise to this solution and it was stirred overnight. Following this incubation period, the reaction mixture was cooled in an ice bath and acidified with 1 N HCl until the pH reached 0. The reaction mixture was concentrated and then dissolved in water. This aqueous solution was then extracted with CH_2Cl_2. The combined organic extracts were washed with 1 N HCl and saturated NaCl, dried with $MgSO_4$, and concentrated to give a white solid. The product was isolated in 69% yield (0.10 g) after column chromatography (~20 mL of silica and a solvent gradient 4:1 hexanes/ethyl acetate to 1:1 ethyl acetate).

IR: 1650, 1693, 3292 cm^{-1}. ^{1}H NMR (500 MHz): δ 1.27–1.32 (m, 1H), 1.52–1.60 (m, 1H), 1.62–1.69 (m, 1H), 1.76–1.81 (m, 1H), 2.37 (m, 2H), 3.08 (m, 2H), 3.45–3.62 (m, 3H), 4.01 (m, 1H), 4.42 (m, 1H), 5.06 (app s, 2H), 5.76 (br s, 1H), 6.32 (br s, 1H), 7.06–7.33 (m, 15H). ^{13}C NMR (125 MHz): δ 32.2, 36.8, 37.9, 38.4, 46.6, 56.8, 58.4, 67.1, 126.0, 127.1, 127.9, 128.2, 128.3, 128.4, 128.5, 128.7, 129.3, 136.0, 136.3, 141.3, 156.2, 172.1. Anal. calcd for $C_{28}H_{32}N_2O_4$: C, 73.02; H, 7.00; N, 6.08. Found: C, 73.15; H, 7.07; N, 6.21.

Compound 5. Ester **19** (50 mg, 0.10 mmol) was dissolved in dioxane (0.37 mL) and flushed under N_2. To this solution was added 0.25 M LiOH (0.4 mL) which had been flushed with N_2. A white precipitate immediately formed and additional dioxane (0.4 mL) and LiOH (0.4 mL) was added to facilitate stirring. After 2 h of stirring at rt, 0.5 N HCl (0.2 mL) was added to quench the reaction. The reaction mixture was diluted in EtOAc and the aqueous layer was extracted further with EtOAc (3×5 mL). The combined organic extracts were dried with $MgSO_4$, and concentrated to give the desired product, which was purified through column chromatography (~2 mL of silica and a solvent gradient from 4:1 to 1:1 hexanes/ethyl acetate) to give 35% yield (17 mg) of analytically pure product.

IR: 1647, 1661, 1697, 3295 cm^{-1}. ^{1}H NMR (500 MHz, acetone-d_6): δ 1.80–1.84 (m, 2H), 2.47–2.60 (m, 4H), 2.94–2.99 (m, 1H), 3.16–3.19 (m, 1H), 4.21 (m, 1H), 4.42 (dd, 1H, J=14.4, 8.3 Hz), 5.02 (m, 3H), 6.51 (d, 1H, J=7.9 Hz), 7.13–7.32 (m, 15H). ^{13}C NMR (125 MHz, acetone-d_6): δ 32.0, 35.8, 38.1, 38.7, 46.2, 56.7, 65.7, 125.6, 126.4, 127.5, 127.6, 128.15, 128.18, 128.2, 128.3, 129.3, 137.2, 137.7, 141.9, 155.8, 170.7, 171.8. FABHRMS: 475.2233 (MH^+, $C_{28}H_{30}N_2O_5$ requires 475.2238).

Compound 6. To a stirred solution of PPh_3 (162 mg, 0.617 mmol) in 1 mL of THF was added diethyl azodicarboxylate (0.97 mL, 0.617 mmol) dropwise. This solution was stirred under N_2 at 0 °C and shielded from light. To this orange solution was added a mixture of alcohol **4** (142 mg, 0.308 mmol) and thioacetic acid (0.088 mL, 1.23 mmol) in 6 mL of THF. This reaction mixture was stirred at 0 °C for 1 h and then gradually warmed up to rt overnight, giving a light pink solution. This solution was concentrated and purified by column chromatography (~2 mL of silica and a solvent gradient 6:1 to 2:1 hexanes/ethyl acetate) to give the thioester in 70% yield (0.112 g).

In a 25 mL Schlenk flask, reagent-grade acetone (3 mL) and 3 M NaOH (3 mL) were subjected to four freeze—pump—thaw cycles to provide strict oxygen-free conditions. Under positive N_2 pressure, the thioester (50 mg, 0.1 mmol) was added as a solid to the Schlenk flask. This reaction mixture was stirred under N_2 for 2 h. A solution of 1 M HCl was added to neutralize the solution. The aqueous layer was extracted with CH_2Cl_2 (3×5 mL) and the combined extracts were dried with $MgSO_4$ and concentrated. This solid was purified through column chromatography (~2 mL of silica and a solvent gradient from 6:1 to 1:1 hexanes/ethyl acetate) to give 28% (13 mg) of desired product.

IR: 1649, 1686 cm^{-1}. ^{1}H NMR (500 MHz): δ 1.47–1.55 (m, 2H), 1.62–1.68 (m, 2H), 1.70–1.77 (m, 1H), 2.39–2.42 (m, 4H), 3.03 (dd, 1H, J=7.9, 13.6 Hz), 3.15 (dd, 1H, J=6.1, 13.6 Hz), 4.04 (m, 1H), 4.35 (dd, 1H, J=7.9, 14.1), 5.06–5.14 (m, 2H), 5.30 (br s, 1H), 5.56 (d, 1H, J=9.3 Hz), 7.07–7.35 (m, 15H). ^{13}C NMR (125 MHz): δ 32.0, 36.7, 38.1, 39.4, 48.1, 56.7, 67.2, 67.9, 125.9, 127.2, 128.1, 128.26, 128.28, 128.4, 128.6, 128.8, 129.3, 136.0, 136.3, 141.3, 156.2, 170.5. FABHRMS: 477.2211 (MH^+, $C_{28}H_{32}N_2O_3S$ requires 477.2200).

High throughput cruzain assay

A fluorometric assay for activity toward cruzain was performed in 96-well microtiter plates. The assay was performed in Dynatech Microfluor fluorescence microtiter plates (opaque white plates), and readings were taken on a Molecular Devices SPECTRAmax Gemini XS Dual scanning microplate spectrofluorometer. The excitation wavelength was 355 nm and the emission wavelength was 450 nm. A 430 nm cutoff filter for emission was used. The peptide substrate Z-Phe-Arg-AMC (Bachem, K_m=1 μM) concentration was 2.5 μM and the cruzain concentration was 0.1 nM. The buffer consisted of a 100 mM solution of pH 5.5 sodium acetate buffer and 1 mM of DTT.

The fluorescent unit readings were taken at ten time points within the linear region of the substrate cleavage, and percentage activity of the enzyme was determined by comparing the change of fluorescent units (FU) for each well against the average change in FU for eight

control wells without inhibitor. All compounds were assayed in duplicate.

Sample procedure. In each well was placed 25 μL of enzyme solution, 125 μL of buffer solution and 10 μL of the inhibitor in DMSO. The compounds were placed only in rows 2–11, with row 12 used for the control wells. Following a 5-min preincubation of the enzyme and inhibitor, 50 μL of the substrate solution was added to each well. The plate was immediately placed into the plate reader and fluorescent readings were taken. The data were analyzed by transferring each plate's readings from the spectrophotometer to EXCEL spreadsheets. An EXCEL macro was written to obtain the slope for each well compared to the slope of the controls. Inhibitors were screened in 2-fold dilutions from 10 μM to 78 nM.

K_i determination

For all inhibitors, the data was fit by nonlinear regression analysis to the equation derived by Williams and Morrison:[14]

$$v = \frac{v_o}{2E_t}\left\{\sqrt{\left[\left(K_i\left(1+\frac{S}{K_m}\right)+I_t-E_t\right)^2+4K_i\left(1+\frac{S}{K_m}\right)E_t\right]}-\left[K_i\left(1+\frac{S}{K_m}\right)+I_t-E_t\right]\right\}$$

For cruzain, the K_m for the substrate was determined to be 1 μM by using a Lineweaver Burke Plot and Eadie—Hofstee Plot. The variables S, E_t, and I_t are the concentrations of substrate, active enzyme, and inhibitor, respectively.

Preparation, purification and crystallization of cruzain bound to inhibitors

Cruzain was expressed and purified as described previously[5,15] [activated cruzain, temporarily 'blocked' with methyl methane thiosulfonate (MMTS) was incubated on ice in solution with 5 mM DTT. The protein solution was buffered in 20 mM bis tris (pH 5.8) with some NaCl (from chromatographic purification]. An excess (1–2 mg) of inhibitor was dissolved in DMSO and added to the protein solution. After stirring for 60 min, the solution was concentrated via vacuum dialysis against a buffer of 2 mM bis tris (pH 5.8) to a final concentration of ~10 mg/mL. Crystals of either **cruz-1** or **cruz-2** were obtained via the hanging drop method against a grid of 0.6–1.0 M sodium citrate (pH 6.6–7.0). Equal volumes of 10 mg/mL protein and sodium citrate solution were mixed and suspended over reservoirs of sodium citrate solution. These drops were allowed to equilibrate at 18 °C for 24 h and subsequently microseeded with existing crystals of cruzain bound to a vinyl sulfone inhibitor.[6] Crystals appeared within 7–10 days of growth at 18 °C.

Data collection, structure solution and crystallographic refinement

All diffraction data were collected at Stanford Synchrotron Radiation Laboratory (SSRL), BL9–1, using monochromatic radiation of 0.98 Å. A MAR345 image plate was used with low temperature conditions of 100 K at the crystal position. Crystals of **cruz-1** and **cruz-2** were flash cooled in liquid nitrogen and mounted in the experimental coldstream for data collection. The structures were solved via molecular replacement using a 1.6 Å model of cruzain (PDB ID 1F2A), without inhibitor or waters. The molecular replacement solution (AmoRe[17]) for **cruz-1** yielded an R_{factor} of 0.377 with a correlation coefficient of 58.0. Similarly, for **cruz-2**, the molecular replacement R_{factor} was 0.381 with a correlation coefficient of 55.7. These statistics indicated that correct solutions had been found. Rigid body refinements, followed by iterative cycles of positional and individual B-factor refinement were completed with XPLOR.[16] Topology, parameter and starting coordinate files for both **1 and 2** inhibitors were generated with the program Moloc.[17] After fitting the inhibitor molecules to their difference electron density in the cruzain active site cleft, water molecules were added automatically using QUANTA (Accelrys, San Diego, CA). Final rounds of high-resolution refinement were performed with SHELX-97,[18] including modeling of anisotropic thermal parameters for all non-hydrogen atoms.

Accession numbers

The coordinates for **cruz-1** and **cruz-2** have been deposited in the Protein Data Bank with accession numbers 1me4 (cruz1) and 1me3 (cruz2), respectively.

Acknowledgements

L. H. and J. A. E. acknowledge support from the NIH (Grant GM 54051) and the Burroughs Wellcome Fund (New initiatives in Malaria Award). L. S. B. acknowledges support from the NIH (AI 35707). Dr. J. H. McKerrow and E. Hansell are also gratefully acknowledged for supplying cruzain, as is Thomas J. Stout for assistance with high-resolution refinement. The Center for New Directions in Organic Synthesis is supported by Bristol-Myers Squibb as a Sponsoring Member and Novartis as a Supporting Member. Portions of this research were carried out at the Stanford Synchrotron Radiation Laboratory, a national user facility operated by Stanford University on behalf of the US Department of Energy, Office of Basic Energy Sciences. The SSRL Structural Molecular Biology Program is supported by the Department of Energy, Office of Biological and Environmental Research, and by the National Institutes of Health, National Center for Research Resources, Biomedical Technology Program, and the National Institute of General Medical Sciences.

References and Notes

1. Amorim, D.; Manco, J. C.; Gallo, L. J.; Marin Neto, J. A. In *Trypanosoma cruzi e doenca de Chagas*; Z. Brener, Z. Arandade, Eds.; Cuanabara Koogan; Rio de Janeiro, 1979; p. 265.
2. Meldal, M.; Svendsen, I. B.; Juliano, L.; Juliano, M. A.; Del Nery, E.; Scharfstein, J. *J. Peptide Sci.* **1998**, *4*, 83.
3. (a) McKerrow, J. H.; Engel, J. C.; Caffrey, C. R. *Bioorg. Med. Chem.* **1999**, *7*, 639. (b) Engel, J. C.; Doyle, P. S.; Hseih, I.; McKerrow, J. H. *J. Exp. Med.* **1998**, *188*, 725.
4. McGrath, M. E.; Eakin, A. E.; Engel, J. C.; McKerrow, J. H.; Craik, C. S.; Fletterick, R. J. *J. Mol. Biol.* **1995**, *247*, 251.
5. Gillmore, S. A.; Craik, C. S.; Fletterick, R. *J. Protein Science* **1997**, *6*, 1603.
6. Brinen, L. S.; Hansell, E.; Cheng, J.; Roush, W. R.; McKerrow, J. H.; Fletterick, R. J. *Structure* **2000**, *8*, 831.
7. Huang, L.; Lee, A.; Ellman, J. A. *J. Med. Chem.* **2002**, *45*, 676.
8. McKerrow, J. H. Personal communication.
9. Engel, J. C.; Doyle, P. S.; Hsieh, I.; McKerrow, J. H. *J. Exp. Med.* **1998**, *188*, 725.
10. Krantz, A.; Copp, L. J.; Coles, P. J.; Smith, R. A.; Heard, S. B. *Biochemistry* **1991**, *30*, 4678.
11. Marquis, R. W.; Ru, Y.; Yamashita, D. S.; Oh, H.-J.; Yen, J.; Thompson, S. K.; Carr, T. J.; Levy, M. A.; Tomaszek, T. A.; Ijames, D. F.; Smith, W. W.; Zhao, B.; Janson, C. A.; Abdel-Meguid, S. S.; D'Alessio, K. J.; McQueney, M. S.; Veber, D. F. *Bioorg. Med. Chem.* **1999**, *7*, 581.
12. Lee, A.; Huang, L.; Ellman, J. A. *J. Am. Chem. Soc.* **1999**, *121*, 9907.
13. Slavíková, B.; Kasal, A.; Budìšínský, M. *Collect. Czech. Chem. Commun.* **1999**, *64*, 1125.
14. Williams, J. W.; Morrison, J. F. *Methods Enzymol.* **1979**, *63*, 437.
15. (a) Eakin, A. E.; McGrath, M. E.; McKerrow, J. H.; Fletterick, R. J.; Craik, C. S. *J. Biol. Chem.* **1993**, *268*, 6115. (b) Eakin, A. E.; Mills, A. A.; Harth, G.; McKerrow, J. H.; Craik, C. S. *J. Biol Chem.* **1992**, *267*, 7411.
16. Brünger, A. T.; Kuriyan, J.; Karplus, M. *Science* **1987**, *235*, 458.
17. Gerber, P. R.; Muller, K. *J. Comput. Aided Mol. Des.* **1995**, *9*, 251.
18. Sheldrick G. M.; Schneider T. R. SHELXL: High Resolution Refinement Sweet, R. M., Carter Jr., C. W., Eds.; In *Methods in Enzymology*; Academic: Orlando, FL, 1997; Vol. 277, p 319.